Early and Late Protective Effect of Bone Marrow Mononuclear Cell Transplantation on Radiation-Induced Vascular Dysfunction and Skin Lesions

Valérie Holler[1], Valerie Buard[1], Telma Roque[1], Claire Squiban[1], Marc Benderitter[1], Stephane Flamant[1], and Radia Tamarat[1]

Abstract

Skin lesions caused by accidental exposure to radiation or by radiotherapy are a major clinical challenge. We evaluated the effect of bone marrow mononuclear cells (BMMNC) on collagen remodeling and vascular function in radiation-induced skin lesions in the acute and late phases in mice. We studied the effect of BMMNC transplantation in a mouse model of cutaneous radiation injury combining local skin gamma-irradiation and biopsy punch wound. Mice were first irradiated, punched and then BMMNC were intramuscularly administered. Seven days after injury, BMMNC promoted wound healing by (i) increasing re-epithelialization, tissue collagen density and mRNA levels of collagens 1A1, 1A2, and 3A1, and (ii) inhibiting the radiation-induced vascular activation and limiting interactions between leukocytes and the vascular endothelium compared with control. Importantly, BMMNC did not amplify the inflammatory response despite the infiltration of neutrophils and macrophages associated with the expression of IL-6 and MCP-1 mRNAs in the tissue. Remarkably, the beneficial effects of BMMNC therapy on matrix remodeling were maintained for 2 months. Furthermore, BMMNC injection restored vascular function in skin tissue by increasing vascular density and vascular permeability. This therapeutic strategy based on BMMNC injection protects against radiation-induced skin lesions by preventing vascular dysfunction and unfavorable remodeling in the acute and late phases.

Keywords

BMMNC, skin, wound healing, irradiation, collagen

Introduction

Wound healing involves the release of factors and the recruitment of inflammatory cell types at the site of injury. It consists of four phases, namely hemostasis, inflammation, tissue formation and tissue remodeling, which overlap in time. The formation of new blood vessels during this process is thought to occur via angiogenesis. Pre-existing microvascular endothelial cells, involved in the induction of microvascular hyperpermeability, cell proliferation and reconstruction of the basement membrane, form new vessels in response to a variety of signaling mechanisms[1,2]. This process is associated with vasculogenesis, involving the recruitment of bone marrow-derived cells and the subsequent incorporation of these cells in the newly forming vessels. Acute radiation skin injury primarily involves cellular alterations and inflammation in the epidermis and dermis. Acute effects begin with erythema, edema, pigment changes and depilation[3]. Severe radiation injury results in complete loss of epidermis and in persistent fibrinous exudates and edema[4]. Chronic radiation skin injury includes delayed ulcers, fibrosis and telangiectasias that present weeks to years after radiation exposure[5]. The effect on wound healing of accidental radiation exposure or of a combination of radiotherapy and surgery is a major clinical challenge, because of synergistic interactions that lead to higher morbidity and mortality than either insult would produce singly.

[1] Institute for Radiological Protection and Nuclear Safety (IRSN), PSE-SANTE, Fontenay aux Roses, France

Corresponding Author:
Radia Tamarat, IRSN, PSE-SANTE, BP17, 92262 Fontenay aux Roses Cedex, France.
Email: radia.tamarat@irsn.fr

Adult stem cells replenish lost cells during wound healing and are key players in tissue regeneration[6,7]. The concept that stem cell injections could be used to reduce normal tissue injury or to stimulate tissue recovery after irradiation has been discussed for a number of years[8]. Several different types of stem cells can be isolated from adult bone marrow. Examples of some of these subpopulations of cells include hematopoietic stem cells, endothelial progenitors and mesenchymal stem cells. Several investigators have chosen to deliver unfractionated bone marrow-derived cells, a technique that has the advantage of minimizing extensive *ex vivo* manipulation of the cells to isolate and expand a selected population of cells. The potential disadvantage of delivering a mixture of cells is that the percentage of cells that are therapeutically useful may be small.

In particular, transplantation of bone marrow mononuclear cells (BMMNC) has been shown to stimulate neovascularization after experimental ischemic injury, resulting in long-term salvage and survival of viable tissue, reduced tissue remodeling and improved organ function[9,10]. We previously showed the beneficial effect of BMMNC in wound healing from radiation exposure[11]. The identification of a central role for BMMNC in tissue revascularization and preservation of function after radiation has renewed the great hope for an efficient pro-remodeling and pro-angiogenic skin therapy with reduced side effects. The use of BMMNC is now being studied in humans, and early small and uncontrolled studies point to a great potential for such therapy in limiting disease progression[12]. However, the safety of BMMNC-based therapy following exposure to radiation is not currently known and has not been tested in experimental studies. Some factors secreted by BMMNC play an important role in neovascularization, such as vascular endothelial growth factor (VEGF), whereas monocyte chemoattractant protein 1 (MCP-1) may potentiate the deleterious skin inflammatory response observed after high-dose irradiation[13]. The maintenance of such a response could contribute to the development and progression of late vascular and tissue radiation damage associated with the inflammatory reaction.

In the present study, we examined the early and late effects of transplantation of BMMNC on the re-epithelialization and vascular dysfunction in radiation-induced skin lesions in mice.

Materials and Methods

Animal Models and Study Protocols

Animal model of irradiation; Wound model; Bone marrow cell transplantation. Wild-type male C57Bl/6 mice, 7 weeks old, (Charles River, Saint Germain sur l'Arbresle, France), were housed four to a cage and received commercial rodent chow and acidified water *ad libitum*. All experimental procedures were approved by the animal care committee of the Institute of Radioprotection and Nuclear Safety and conformed to the

French regulations for animal experimentation (Act no. 2001-464, May 29 2001).

Two days before irradiation, mice weighing 19–22 g were anesthetized by spontaneous inhalation of isoflurane-N_2O (F_iO_2 0.35, 0.015L/L Aerrane, isoflurane, Baxter S.A.S., Maurepas, France). The entire back was shaved and remaining roots were removed with hair depilatory cream on each mouse (Veet, Reckitt Benckiser, Massy, France). Prior to irradiation, mice were anesthetized by intraperitoneal injection of a mixture of ketamine (100 mg/kg, Virbac France, Carros, France) and xylazine (10 mg/kg, Rompun, Bayer Healthcare, Puteaux, France). Mice were laid on a Polymethyl Methacrylate (PMMA) device (Leroy Merlin, France); the dorsal skin was gently stretched and maintained with two suturing lines (Vicryl, Ethicon, Johnson-Johnson Intl, Belgium). The area of the dorsal skin exposed to the ionizing radiation was 2 cm $\times$ 4 cm. Irradiation was given as a local single exposure (20 Gy; 1.5 Gy/min) using 1.25 MeV γ-rays of a collimated ^{60}Co source (ICO 4000, IRSN, Fontenay aux roses, France). The reference dose rate was established with a PTW ionization chamber (PTW, Freiburg, Germany) in realistic irradiation conditions in air on the PMMA plate with a tissue-equivalent phantom at mouse body position to generate retro-scattered radiation from the mice bodies. The ionization chamber of 0.125 cm^3 was calibrated in term of tissue kerma at IRSN reference ^{60}Co facility (accredited metrological unit SMH no. 2-1612 – COFRAC accreditation, France). Sham-irradiated mice were handled like irradiated mice but were not exposed to the radiation source. Immediately after irradiation, an excisional 8 mm full-thickness skin wound was created on the midline of the dorsal skin using a sterile biopsy punch. The wound was left uncovered. Suspensions of BMMNC and phosphate-buffered saline (PBS) were intramuscularly injected all around the wound. Five groups were formed (n = 12–15 mice per group): non-irradiated and non-punched (NIR-NP), irradiated and non-punched (20 Gy NP); non-irradiated and punched (NIR-P), irradiated and punched (20 Gy P); and irradiated, punched and treated mice (20 Gy P+BMMNC). An overview of animal groups and measurements is described in Supplemental Table 1, available online.

Mice were observed daily until day 60 following radiation exposure.

Bone marrow cell isolation. Bone marrow cells were isolated by flushing tibias and femurs of C57Bl/6 mice. Low-density mononuclear cells were then isolated by density gradient centrifugation with Ficoll (Sigma-Aldrich, Saint-Quentin Fallavier, France). BMMNC (1 $\times$ 10^6 cells/100 µl of PBS) were intramuscularly administered just after BMMNC isolation in each animal immediately after wounding.

Intravital microscopy. Mice were anesthetized by intraperitoneal injection of 2.5% tribromoethanol (0.15 mL/10 g body weight, Sigma-Aldrich) and leukocytes were stained by

intravenous administration of 10.4% rhodamine 6G (62.5 µl/mouse, Sigma-Aldrich). The mice were maintained at 37°C on a heating-pad during the whole experiment. A dorsal skin flap was dissected free from the body and was placed in a 5% gelatin-coated PMMA chamber for observation of the dorsal microcirculation (Sigma-Aldrich). By preserving all the vessels at one side of this flap from the cranial side to the caudal side, blood circulation was maintained in this part and allowed visualization and quantification of leukocyte–endothelial interactions. Following 5-min stabilization after intravenous injection of rhodamine 6G, 50–100 µm diameter venules were selected for direct observation of leukocyte–endothelium interactions as previously described[13].

Two parameters of leukocyte–endothelium interactions were measured using intravital microscopy: (1) the mean leukocyte rolling velocity and (2) the number of rolling leukocytes. Leukocyte–endothelial interactions were quantified using the software Histolab 4.3.6. Leukocyte–endothelial interactions were analyzed for 1–4 minutes per vessel within a square of 25×25 µm^2, 50×50 µm^2 or 100×100 µm^2 depending on the vessel diameter, and quantifications were normalized thereafter per min/0.01 mm^2. Experiments were performed on 4–5 animals per group, and 3–5 vessels per animal were quantified.

Skin vascular permeability. To quantify vascular leakage in the dorsal skin venules 60 days after irradiation, with or without BMMNC injection, 25 mg/kg fluorescein isothiocyanate (FITC)-labeled 77-kDa dextran (Sigma-Aldrich) was administered intravenously to anesthetized mice. Blood vessels were visualized with a fluorescence inverted microscope (Nikon, Champigny sur Marne, France). Fluorescence intensity was recorded 1–30 minutes after FITC-dextran injection with an Exwave HAD digital color camera (Sony, Microvision Instruments, Evry, France). Fluorescence intensity was quantified using the software Histolab 4.3.6 (Microvision Instruments, Evry, France) and was measured within the vessel under study (I int) and in a contiguous area of perivascular interstitium (I ext). Background fluorescence intensity (Bg) was subtracted from each value. An index of vascular leakage (IP) was calculated by dividing (I ext – Bg) by (I int – Bg)[14]. Experiments were performed on three animals/group and 30 vessels/animals were analyzed for the calculation of the permeability index. Sampling area was proximal to the punch lesion where skin was irradiated.

Multiphoton microscopy (second harmonic generation). Mouse skin tissue was embedded in an optimum cutting temperature compound (OCT, Tissue-Tek, Sakura Finetek, Zoeterwoude, The Netherlands), frozen in liquid nitrogen and stored at –80°C. Then cryo-samples were cut into 250–300 µm-thick sections for imaging. Skin samples of each group were imaged using a multiphoton confocal microscope (LSM 780 NLO, Carl Zeiss Microimaging, Le Pecq, France). Images of collagen fiber orientation, distribution and intrinsic fiber structure from the dermis were collected using a Plan-Apochromat 20× (1.0-NA) water immersion objective lens (Carl Zeiss). A tunable titanium/sapphire femtosecond laser (Chameleon, Coherent, Courtaboeuf, France) was used to excite the specimen. Second harmonic generation signals for collagen were collected at 800 nm.

Quantitative Histopathology, Immunohistochemistry Methods and Morphometry

Vascular network. A macrophotograph of each skin flap was taken and analyzed by Histolab 4.3.6 in order to quantify the vascular area around the punch (the vascular area was expressed as the area occupied by vessels in the same quantification area in all conditions) and the number of vascular segments (nonbranching blood vessel)[15].

Skin biopsies. Two skin samples per mouse were taken as 8 mm × 16 mm biopsies from the center of the skin flap and corresponding to the central area of the lesion. Each skin sample was cut into two equal parts (8 × 8 mm) through the center of the wound. The first sample was fixed in 4% formaldehyde and embedded in paraffin for histological assessments and immunohistochemistry (4–7 mice per group). Two samples (for leukocyte staining and multiphoton experiments) were embedded in Tissue-Tek OCT compound (Sakura Finetek), snap-frozen in liquid nitrogen and stored at –80°C for immunolabeling. The last sample was stored in RNA later solution (Qiagen, Courtaboeuf, France) for RNA extraction.

Analyses of re-epithelialization. The paraffin-embedded skin was cut into 5 µm sections, deparaffinized, hydrated, dehydrated and stained with haematoxylin, eosin and safran (HES, Sigma-Aldrich) for histological examinations. Width of the wound and distance of the traversed epithelium was measured at day 7 by capturing images of HES-stained sections from a Zeiss Axiophot microscope using a video color camera (JVC KY-F75U, Carrières sur Seine, France) and was measured using Histolab 4.3.6.

Collagen histochemical analysis. Sections were stained with Sirius red to evaluate collagen content (Sigma-Aldrich). Collagen was quantified by image analysis using Histolab 4.3.6.

Immunohistochemistry labeling. Polyclonal rat anti-mouse-CD45 IgG antibody (BD Pharmingen, San Jose, CA, USA) was used at 1/2000 to identify leukocytes. Quantification of leukocytes was expressed as the number of CD45-positive cells per square millimeter of tissue.

Immunohistochemical staining using rat anti-mouse CD62E (E-selectin) IgG antibody (1/2000, BD, USA), goat anti-mouse CD54 (ICAM-1) IgG antibody (1/200, R&D Systems, Lille, France), rat anti-mouse F4/80 (1/500, Tébu-Bio, Le Perray en Yvelines, France) and rat anti-mouse CD31 (1/100, Millipore, Mosheim, France) was performed on frozen skin sections. Mouse secondary antibodies were then used at a dilution of 1/200 (alexa 488 goat anti-rat,

alexa 488 rabbit anti-goat and alexa 568 goat anti-rat, Molecular Probes, Saint Aubin, France). Specificity of immunohistochemical staining was demonstrated by the absence of staining products using a non-immune corresponding immunoglobulin. The number of vessels positive for CD31, F4-80, E-selectin and ICAM-1 was qualitatively determined by image analysis using Histolab 4.3.6.

RNA Isolation and RT Real-Time Quantitative PCR. Total RNAs were isolated from skin biopsies using RNeasy Fibrous Tissue Mini Kit (Qiagen), according to the manufacturer's recommendations. Total RNA integrity was analyzed using Agilent 2100. After quantification on a NanoDrop ND-1000 apparatus (Nanodrop Technologies, Rockland DE, USA), 1 μg of total RNA was used for reverse transcription (RT) using the High Capacity Reverse Transcription Kit (Life Technologies, Paisley, UK) according to the manufacturer's instructions. PCR amplification was performed using Taqman PCR master Mix (Life Technologies) with the ABI PRISM 7900 Sequence detection system (Life Technologies).

TaqMan gene expression assays were used as follows: Coll1a1 (Mm00801666_g1), Coll1a2 (Mm00483888_m1), Coll3a1 (Mm00802331_m1), ICAM-1 (Mm00516023_m1), IL6 (Mm00446190_m1), IL10 (Mm00439616_m1), MCP1 (Mm00441242_m1). To calculate relative gene expression levels between different samples, we used the threshold cycles (Cts) normalized to the Ct of GAPDH as an internal control (TaqMan® Rodent GAPDH, Life Technologies). Relative mRNA quantification was performed by using the comparative $\Delta\Delta$CT method.

Data analysis. Results are presented as means $\pm$ SEM (standard error of the mean). One-way analysis of variance (ANOVA) was used to compare each parameter. Post hoc Tukey or Dunn tests were then performed to identify which group differences account for the significant overall ANOVA (Sigma Plot 11.0, Jandel Scientific, Systat software, San Jose, CA, USA). Differences were accepted as statistically significant at $p < 0.05$.

Results

BMMNC Promoted Wound Healing and Re-Epithelialization at Day 7 after Skin Radiation Injury

The rate of wound healing was significantly increased following BMMNC injection, as previously described[11]. Irradiation tended to increase wound size compared with non-irradiated (NIR) mice from 2636 $\pm$ 422 μm to 3347 $\pm$ 251 μm, whereas re-epithelialization increased markedly in BMMNC-injected mice compared with untreated mice (Fig. 1A), leading to a reduction in scar size ($p < 0.001$; Fig. 1B).

Changes in skin re-epithelialization were associated with a modification in tissue collagen content. Collagen levels quantified by Sirius red staining tended to decrease after irradiation, while BMMNC administration tended to increase collagen levels by 1.3-fold compared with untreated mice, though not significantly (collagen density: 0.51 $\pm$ 0.07 vs. 0.65 $\pm$ 0.03) (Fig. 1C, D). In order to get more detailed information about the matrix network of the dermis, we took advantage of collagen fiber effectiveness in second harmonic generation (SHG) and performed collagen analysis by multiphoton microscopy (Fig. 1E, F). Collagen density was significantly decreased by 1.8-fold after radiation dermal incision compared with NIR mice (collagen density: 0.81 $\pm$ 0.04 vs. 0.45 $\pm$ 0.05; $p < 0.001$), whereas BMMNC injection resulted in significantly increased collagen deposition by 1.4-fold compared with untreated animals (collagen density: 0.45 $\pm$ 0.05 vs. 0.61 $\pm$ 0.03; $p < 0.05$) (Fig. 1G, left). In addition, the mean diameter of collagen fibers was significantly reduced by 1.3-fold after dermal incision compared with uninjured mice (mean diameter: 7.77 $\pm$ 0.20 μm vs. 5.94 $\pm$ 0.19 μm; $p < 0.001$), with no additional effect after irradiation (Fig. 1G, right). In contrast, the mean fiber diameter was significantly increased in BMMNC-injected mice compared with untreated animals (6.08 $\pm$ 0.16 μm vs. 6.96 $\pm$ 0.19 μm; $p < 0.01$). Interestingly, irradiated mice displayed reduced tissue expression of collagen 1A1, 1A2 and 3A1 mRNAs compared with NIR animals, which was also observed in BMMNC-injected animals. Finally, no effect of the BMMNC administration on the mRNA collagen expression was observed (Fig. 1 H).

BMMNC Inhibited the Radiation-Induced Vascular Activation at Day 7

We previously showed that high-dose skin irradiation induced endothelium activation[13]. Intravital microscopy analysis of the interactions between leukocytes and endothelial cells around the dermal incision (Fig. 2A*ii–iv*) revealed a significant 1.3-fold reduction in leukocyte rolling velocity after irradiation compared with NIR mice, in non-punched (NP) conditions, though the number of rolling leukocytes remained unaltered (Fig. 2B).

In the punched (P) condition, we found a similar reduction in the rolling velocity for both irradiated and NIR animals compared with control NP mice. More importantly, BMMNC injection restored basal rolling velocity values similar to NIR-NP mice (Fig. 2B). In addition BMMNC-injected mice displayed an increased vascular density, as evaluated by CD31 immunohistochemistry (Fig. 2A*i*). Altogether, these results suggest that BMMNC inhibit irradiation-induced acute vascular activation by reducing the strength of the interactions between leukocytes and the endothelium.

BMMNC did not Exacerbate the Inflammatory Response at Day 7

Similar to our previous study[13], semi-quantitative analysis of immunostained tissue showed a massive infiltration of
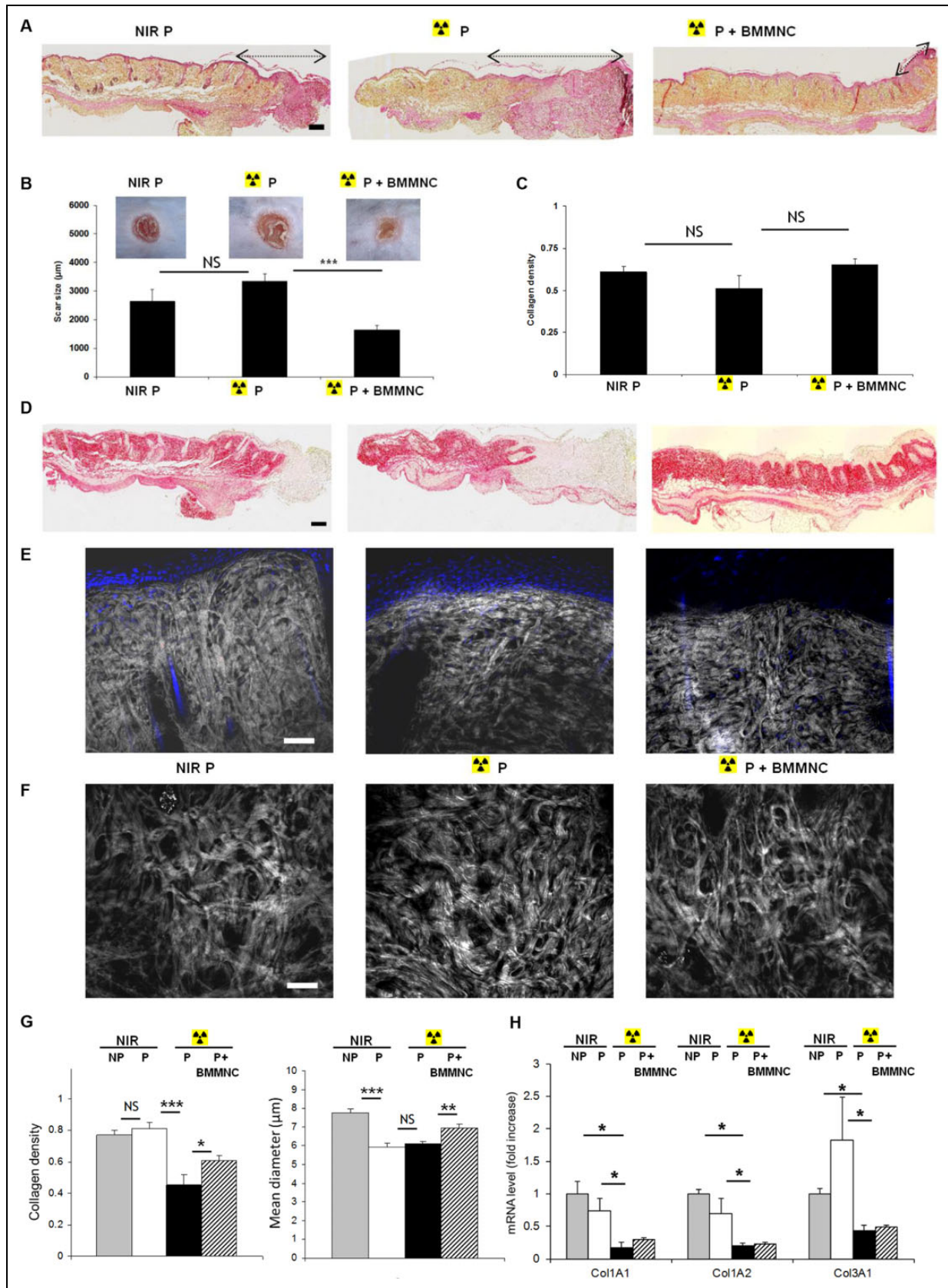
Figure 1. Characterization of the cutaneous radiation model at day 7 after skin injury and BMMNC injection. A: For 3 conditions after skin punch (P): non-irradiated (NIR-P), 20 Gy irradiated (20 Gy P) and 20 Gy irradiated + BMMNC injection (20 Gy P + BMMNC). Representative half HES-stained section of mouse dorsal skin 7 days after irradiation (original magnification ×5; scale bar: 200 μm). Re-epithelialization

inflammatory leukocytes (CD45+) and macrophages (F4/80+) in the skin following irradiation (Fig. 2C, D). Interestingly, skin tissue inflammation in BMMNC-injected mice was similar to untreated animals (Fig. 2C, D). Furthermore, the radiation-induced inflammatory infiltrate was accompanied by increased tissue gene expression of IL-6 and MCP-1 by 1.8- and 2.5-fold, respectively, compared with NIR mice ($p < 0.05$ and $p < 0.01$, respectively; Fig. 2E). However, no modifications in gene expression were observed after BMMNC injection compared with irradiated mice. In addition, no changes were noted in ICAM1 or IL-10 gene expression levels in either group. These results suggest that BMMNC injection does not exacerbate the acute radiation-induced inflammatory response.

BMMNC Effect on Matrix Remodeling 60 Days after Skin Injury

As shown in Fig. 3A, 60 days after irradiation, wound closure was largely completed. Sirius red staining and SHG microscopy analyses indicated that collagen levels were still significantly reduced by 1.4-fold and 1.3-fold, respectively, in irradiated mice compared with NIR animals ($p < 0.05$) (Fig. 3B–D). However, BMMNC treatment led to an increase in collagen density compared with untreated animals ($p < 0.01$), reaching levels similar to control NIR mice (Fig. 3C, D). Moreover, the mean collagen fiber diameter was still significantly reduced in punched animals compared with control mice (8.65 ± 0.22 μm vs. 5.08 ± 0.13 μm, $p < 0.001$), while it was slightly, yet significantly, increased in the irradiated group, and to a larger extent in BMMNC-injected mice (5.08 ± 0.13 μm vs. 5.98 ± 0.15 μm vs. 7.04 ± 0.19 μm, respectively, $p < 0.001$) (Fig. 3D, right). In addition, irradiated mice displayed reduced tissue expression levels of collagen mRNAs compared with NIR animals, which were reverted in BMMNC-injected mice (Fig. 3E).

BMMNC Inhibited the Radiation-Induced Vascular Activation at Day 60

In agreement with our previous study[13], the leukocyte rolling velocity was still significantly reduced in both groups of irradiated animals (P and NP; Fig. 4B, right and online supplemental video S1-S2), accompanied by an increased number of rolling leukocytes compared with NIR controls (41 vs. 128 R/min/0.01mm^2, $p < 0.05$) (Fig. 4A and B, left). This observation confirms the sustained vascular activation state over a period of 60 days following irradiation. Strikingly, BMMNC-injected mice showed values of rolling velocity similar to controls, compared with untreated animals (73.4 ± 3.2 μm/s vs. 102.7 ± 5.2 μm/s, $p < 0.01$), together with a reduced number of rolling leukocytes (128 vs. 75 R/min/0.01mm^2 $p < 0.05$) (Fig. 4B and online supplemental video S3). Altogether, these results suggest that a single BMMNC injection exerts long-lasting effects in preventing radiation-induced cutaneous vascular activation.

BMMNC Effect on the Inflammatory Response at Day 60

A sustained inflammatory infiltrate including CD45+ leukocytes and F4/80+ macrophages was still observed in the skin 60 days post-radiation injury, with moderate increase of CD45 labeling in BMMNC-injected mice estimated by semiquantitative analysis of immunostained tissue (Fig. 4C, D).

A sustained inflammatory reaction was still observed in the late phase of the BMMNC-injected animals. Furthermore, although tissue expression levels of IL-6, IL-10, ICAM1 and MCP-1 genes were similar between irradiated and NIR mice, the BMMNC-injected animals showed increased levels of MCP-1 mRNA, and a mild, nonsignificant increase of IL-10 and IL-6 mRNAs, compared with untreated mice (Fig. 4E).

BMMNC Restored the Vascular Function at Day 60

We found that skin vascular density, as defined as the area occupied by vessels relative to total quantification area[15], was unchanged upon radiation exposure (Fig. 5A, left), while the number of vascular segments was significantly reduced (Fig. 5A, right), indicating persisting vasodilation 60 days post-irradiation in both P and NP groups. In contrast, BMMNC-injected mice displayed markedly reduced vascular area compared with untreated animals (Fig. 5A, left), accompanied by an increase in the number of vascular segments (Fig. 5A, right), suggesting increased angiogenesis with an inhibition of vascular dilation. These effects were illustrated using the CD31 marker (Fig. 5B).

Figure 1. (Continued). was measured as the distance the newly formed epidermis migrated (dotted arrow) into the center of the wound bed in each group ($n = 7$). B: Top: representative photomicrographs of the dorsal skin punch wound healing in the three groups 7 days after injury ($n = 7$). Bottom: quantification of dorsal scar size from HES-staining sections ($n = 7$). C: Quantification of collagen density from Sirius red-stained sections ($n = 4$). D: Photomicrographs of Sirius red-stained sections of the dorsal skin; red staining intensity corresponds to the amount of collagen deposition (original magnification ×5; scale bar: 200 μm). E, F: Multiphoton imaging of the collagen network of the upper (E) and reticular (F) dermis of the dorsal skin (original magnification ×20; scale bar: 50 μm, blue: dapi; gray: SHG signals). G: Left: quantification of SHG pictures: collagen density. Right: mean diameter of the collagen fibers ($n = 3$). H: Quantitative PCR analysis of skin mRNA levels of collagens 1A1, 1A2 and 3A1 ($n = 3$). Results are shown as fold change of expression compared with skin tissue from non-irradiated, non-punched animals (NIR-NP), set to 1. Data are expressed as the mean $\pm$ SEM; ***$p < 0.001$, **$p < 0.01$, *$p < 0.05$ relative to NIR group or the untreated group, NS: not significant.
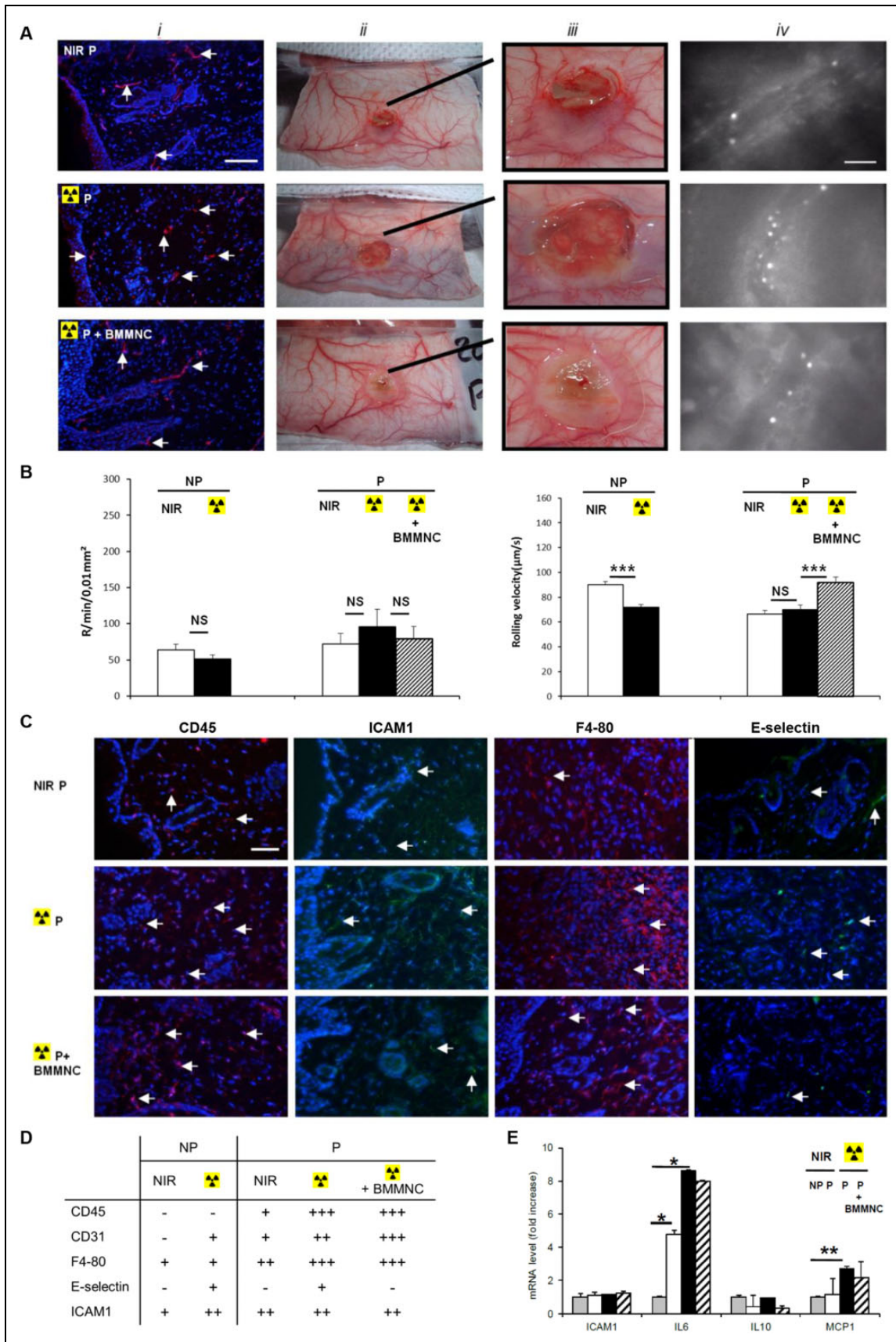
Figure 2. The vascular network in the wound healing process 7 days after skin injury and BMMNC injection. A: (*i*) Representative immunohistochemical analysis of CD31 (red) in the dorsal skin (arrow; original magnification ×20; scale bar: 100 μm). (*ii*) Vascular network

These observations suggest a sustained beneficial effect of BMMNC injection on vascular function in late phase in irradiated conditions. Moreover, our data demonstrated that BMMNC injection resulted in a mild, yet significant increase of vascular permeability at 1, 10, 20 minutes and 30 min after dextran-FITC injection compared with untreated animals (Fig. 5C and D).

Discussion

The main objective of this study was to demonstrate the beneficial role of BMMNC administration in remodeling processes and in repair of radiation-induced vascular damage in the acute and late phases. Further, we demonstrated that BMMNC injection in irradiated skin lesions does not heighten the inflammatory response to irradiation.

In the present study, we underlined the beneficial effect of BMMNC on re-epithelialization and wound healing in irradiated conditions. Collagen density in skin tissue decreased 7 days after irradiation, compared with NIR tissue, in association with a decrease in collagen fiber diameter, as measured by SHG microscopy. Moreover, these results were associated with a decrease in the expression of three collagen genes: col1A1, col1A2 and col 3A1. This decrease in collagen component was maintained 60 days after irradiation. Importantly, we found that BMMNC administration restored the collagen density and mean fiber diameter, together with a tendency to upregulate collagen genes expression in the skin tissue at day 60. These observations are in accordance with studies showing that fibroblasts and myofibroblasts from irradiated tissue exhibit abnormalities in collagen production and contractile properties and may be permanently altered by radiation[16,17]. They do not produce sufficient collagen to keep up with the demands of wound healing, or the collagen that is produced does not mature quickly enough to meet these demands during the acute phase of wound healing. In a wound healing model of 18 Gy-irradiated guinea pigs, Bernstein et al. demonstrated a downregulation of gene expression of the A1 chain of type 1 collagen in wounds 7 days after irradiation[18]. Similarly, in a clinical study of irradiated breast cancer, using scanning electron microscopy, thinner fibers were observed in the irradiated skin[19]. Finally, our data are in accordance with other studies showing that transplantation of fibroblasts in both irradiated and NIR settings partially restores wound healing[20,21].

Leukocyte recruitment is a multistep process, which includes leukocyte rolling, activation, firm adhesion to the endothelium and leukocyte infiltration in the tissue. It contributes to the first step in the inflammatory response[22,23]. We previously showed that endothelium activation after irradiation is deleterious for vascular function and contributes to skin pathogenesis and deleterious effects in the short and long term[13]. In the present study we demonstrated that BMMNC administration following radiation injury prevented radiation-induced endothelium activation, associated with an increase in leukocyte rolling velocity in the skin lesion 7 days post-injury. Furthermore, we observed that the BMMNC protective effect against endothelial activation was sustained for at least 60 days after irradiated skin injury. These data suggest that a single BMMNC injection results in acute and long-lasting inhibition of radiation-induced endothelial activation.

The vascular dysfunction observed *in vivo* after irradiation is in agreement with the early vascular activation and cell surface expression observed after the dorsal irradiation of NP skin murine model[13] and *in vitro* in skin organ cultures and cultured human dermal microvascular endothelial cells[24]. Therefore, a significant increase in leukocyte rolling and adherence to the endothelium of the vascular wall was noted following irradiation of rat skin-fold window chambers[25]. Moreover, vascular dysfunction was associated with downregulation of nitric oxide (NO) expression in the blood vessels and with a decrease in cytokines and expression of adhesion molecule[13].

A previous study has demonstrated that the administration of BMMNC induces immediate endothelial nitric oxide synthase (eNOS)-dependent vasodilation in ischemic femoral arteries[26]. In fact, it has also been shown that NO regulates leukocyte trafficking by preventing leukocyte adherence to the endothelium[27,28]. Recruitment of monocytes triggered by MCP-1 was shown to induce arteriogenesis at inflammatory ischemic sites[29]. Because BMMNC contain monocyte-lineage progenitor cells, we hypothesized that the injection of BMMNC could contribute to the development and the progression of late tissue and vascular radiation damage. Our results indeed confirmed that leukocyte and macrophage accumulation in the skin tissue at day 7 post-irradiation was maintained, yet not increased by BMMNC injection in the wound area. In addition, irradiation induced expression of IL-6 and MCP-1 in the tissue 7 days

Figure 2. (Continued). of the dorsal skin flap where intravital experiments were performed. (*iii*) Magnification of the punched area. (*iv*) Visualization by intravital videomicroscopy of leukocyte–endothelium interactions in the dorsal skin vessels around the punch after intravenous administration of rhodamine 6G (original magnification ×40; scale bar: 50 μm). B: The number of rolling leukocytes (R) per min per 0.01 mm^2 (left) and the rolling velocity (right) were determined by intravital microscopy 7 days post-injury around the skin lesion. Data are expressed as the mean ± SEM (0 Gy: $n = 4$ mice; 20 Gy: $n = 5$ mice). C: Representative immunohistochemical analysis of CD45 (red), ICAM1 (green), F4-80 (red) and E-selectin (green) in the dorsal skin (arrows; original magnification ×20; scale bar: 100 μm). D: Qualitative observation of 10 fields for each mouse of each group for CD45, CD31, ICAM1, F4-80 and E-selectin labeling ($n = 3$). E: Quantitative PCR analysis of skin tissue mRNA levels of ICAM1, IL6, IL10 and MCP1 ($n = 3$). Data are expressed as the mean ± SEM. ***$p < 0.001$, **$p < 0.01$, *$p < 0.05$ relative to the NIR group or to the untreated group, NS: not significant.
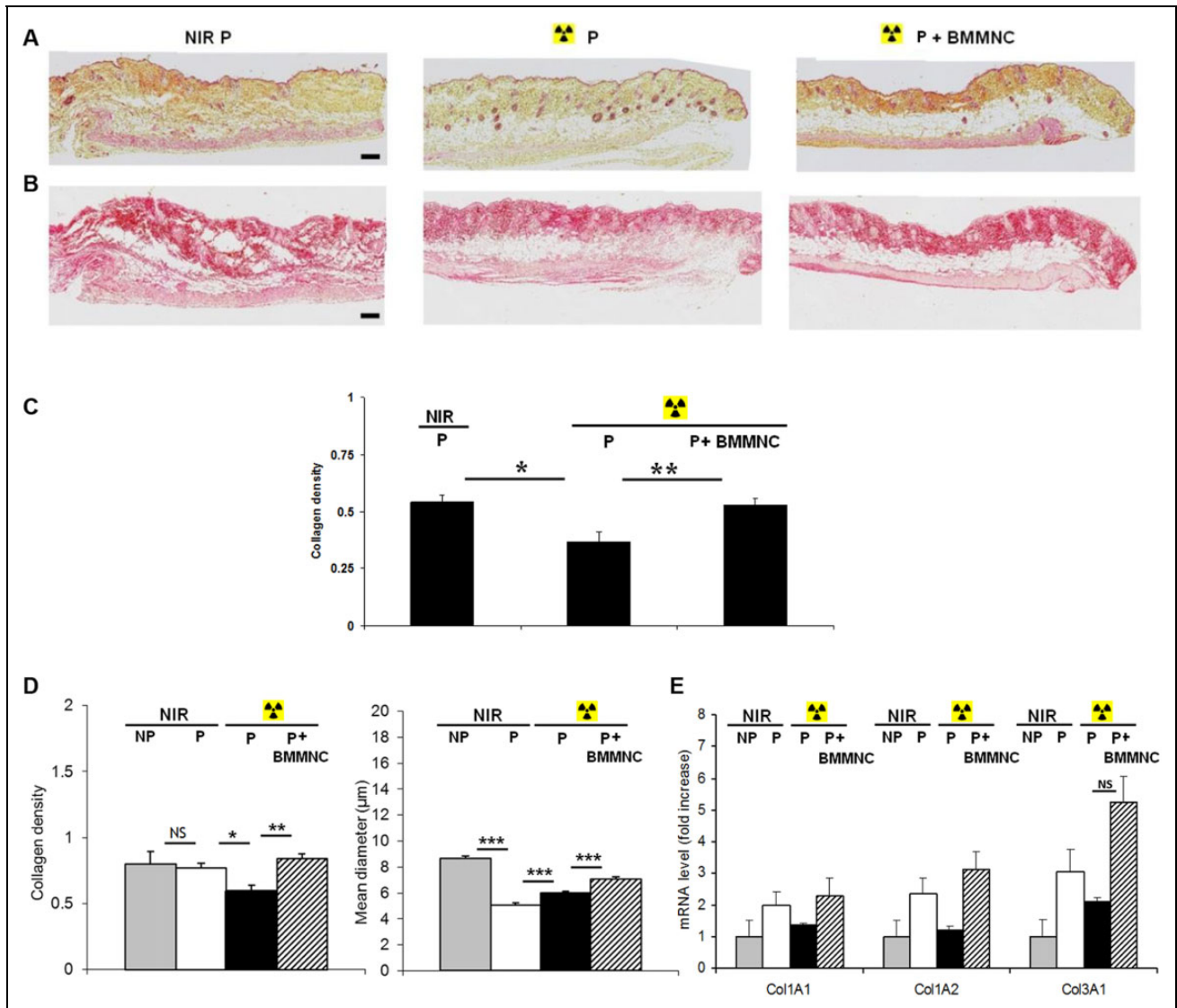
Figure 3. Characterization of the cutaneous radiation model at day 60 after skin injury and BMMNC injection. A, B: Photographs of HES (A) and Sirius red (B) -stained sections of the dorsal skin of mice (original magnification ×5; scale bar: 200 μm). C: Quantification of collagen density from Sirius red-stained sections shown in (B) ($n = 5$). D: Quantification from SHG pictures: collagen density and mean collagen fiber diameter ($n = 3$). E: Quantitative PCR analysis of skin mRNA levels of collagens 1A1, 1A2 and 3A1 ($n = 3$). Data are expressed as the mean ± SEM; ***$p < 0.001$, **$p < 0.01$, *$p < 0.05$ relative to the NIR group or the untreated group, NS: not significant.

after skin injury, which is in agreement with an increase in neutrophil and macrophage infiltration. Interestingly, BMMNC therapy did not heighten this cytokine secretion and consequently the inflammatory reaction. Surprisingly, we observed that BMMNC administration resulted in increased tissue expression of IL-6 and MCP-1 after 2 months, associated with neutrophil and macrophage infiltration in the tissue.

Our results show that vascular dysfunction induced by local irradiation of the skin is maintained for at least 2 months after skin injury. Furthermore, we show that there is a downregulation of the number of vascular segments counted around the skin injury, associated with low levels of CD31 expression

in the skin lesion compared with NIR animals. More importantly, BMMNC administration restored vascular function in the skin after irradiation and induced hyperpermeability, which is required for angiogenesis[26]. These results are in agreement with previous reports showing that BMMNC induce vasodilation of pre-existing vascular networks and increase vascular permeability, which are both crucial to BMMNC-stimulated neovascularization[26].

Our results show that BMMNC have a beneficial effect on radiation-induced vascular function late in the course of injury. These findings are in accordance with the identification of a central role for BMMNC in tissue revascularization and in preservation of function in radiation-induced vascular
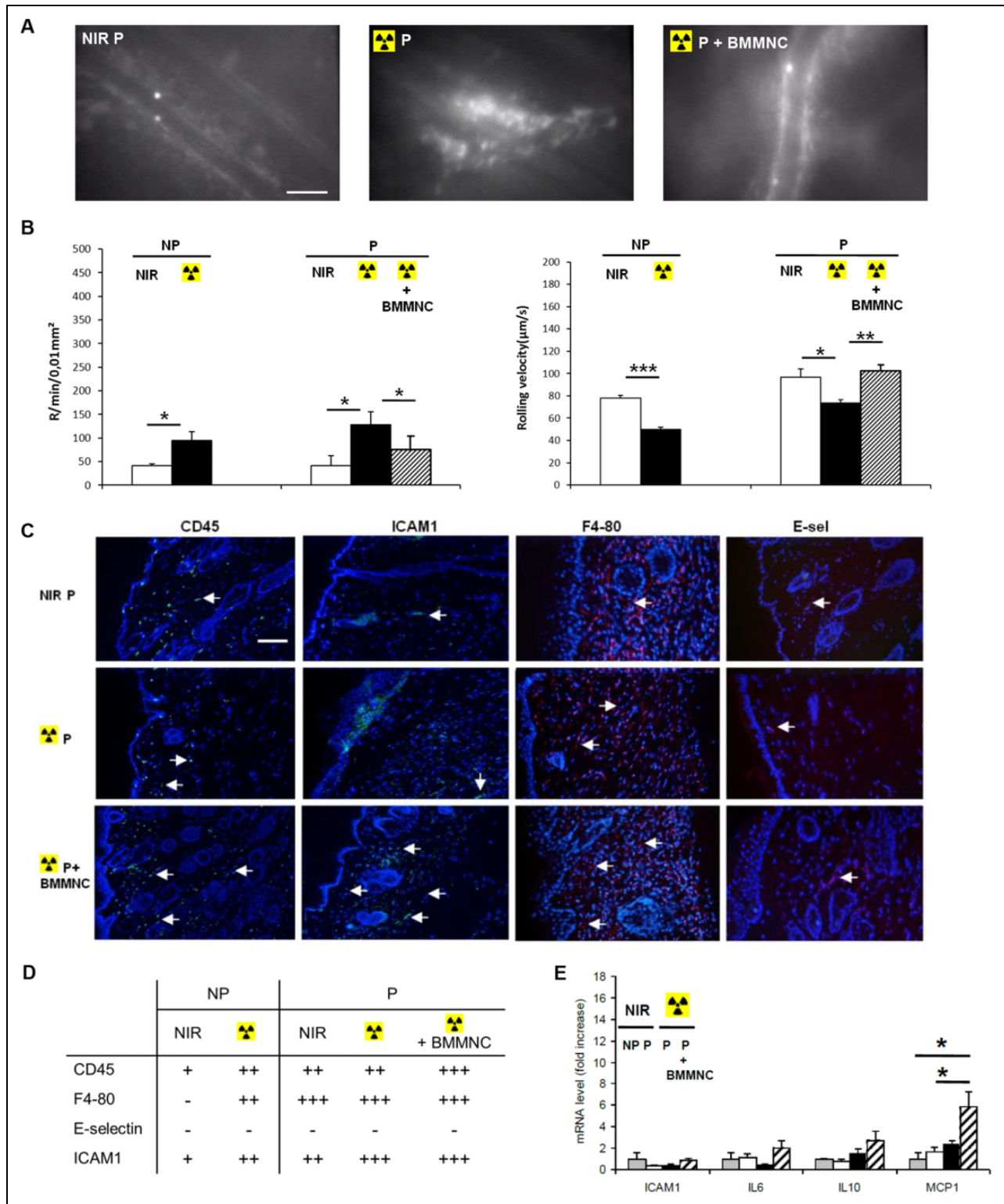
Figure 4. The vascular network in the wound healing process 60 days after skin injury and BMMNC injection. A: Visualization by intravital videomicroscopy of leukocyte–endothelium interactions in the dorsal skin vessels around the punch after intravenous administration of rhodamine 6G (original magnification ×40; scale bar: 50 μm). B: The number of rolling leukocytes (R) per min per 0.01 mm² (left) and the rolling velocity (right) were determined by intravital microscopy around the area corresponding to the injured site. Data are expressed as the mean ± SEM ($n = 5$ mice). ***$p < 0.001$, **$p < 0.01$, *$p < 0.05$ relative to the NIR group or to the untreated group, NS: not significant. C: Representative immunohistochemical analysis of CD45 (red), ICAM1 (green), F4-80 (red) and E-selectin (red) in the dorsal skin ($n = 3$; original magnification ×20; scale bar: 100 μm). D: Qualitative observation of 10 fields for each mouse of each group for CD45, ICAM1, F4-80 and E-selectin labeling ($n = 3$). E: Quantitative PCR analysis of skin tissue mRNA levels of ICAM1, IL6, IL10 and MCP1 ($n = 3$). Data are expressed as the mean ± SEM; *$p < 0.05$.
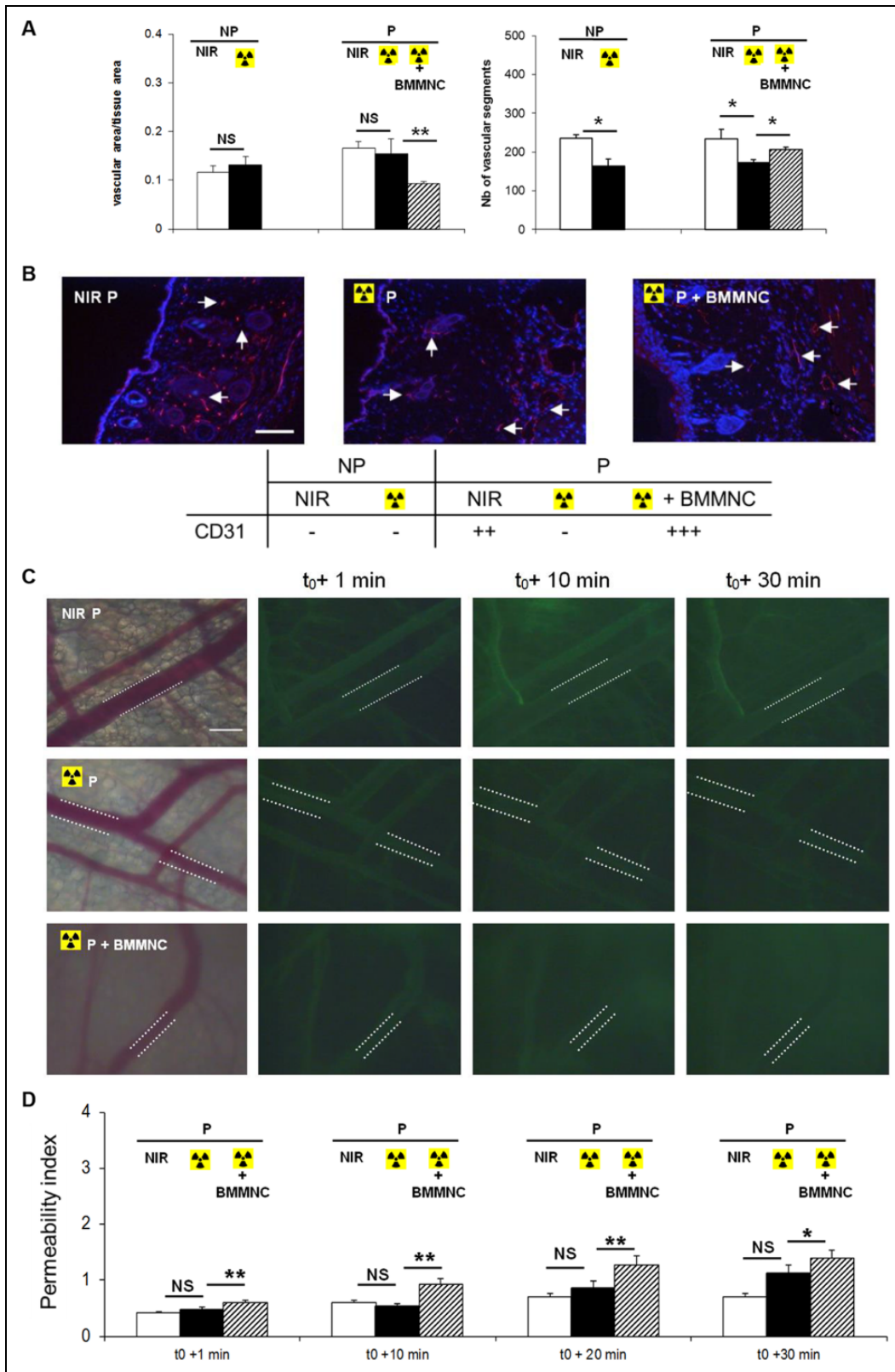
Figure 5. Evaluation of the vascular function 60 days after skin injury and BMMNC injection. A: Left: quantification of the vascular density or area occupied by vessels per unit area was quantified by image analysis of the dorsal skin. Right: the number of vascular segments in the same area was quantified by manual counting ($n = 3$). B: Representative immunohistochemical analysis of CD31 (red) in the dorsal skin (arrow; original magnification ×20; scale bar: 100 μm) and qualitative observation of 10 fields for each group ($n = 3$). C: FITC-dextran leakage from dorsal skin venules was evaluated for 30 minutes (original magnification ×20; scale bar: 100 μm). D: Quantification of the permeability index as a function of time ($n = 3$). Data are expressed as the mean ± SEM; **$p < 0.01$, *$p < 0.05$.

damage, which has renewed hope for an effective proangiogenic therapy with reduced side effects[30].

Finally, it is likely that the overall biological effects of BMMNC result from the synergistic interactions of the multiple components of the BMMNC on multiple signaling pathways. Three types of multipotent bone marrow-derived cells have been shown to have significant therapeutic potential in tissue regeneration: hematopoietic stem cells, mostly myeloid progenitors, mesenchymal stem cells (MSC), and endothelial progenitor cells (EPC). In our skin injury model we have previously shown that EPC stimulated the neovascularization process[31] and MSC isolated from the bone marrow increased the wound healing process, associated with immunomodulatory effects[6]. Regarding the literature, we can consider that we will have a beneficial effect provided by the immunomodulatory function of MSC on the radiation-induced skin injury. In order to highlight the role of the inflammatory cells supplemental experiments based on administration of BMMNC depleted in CD4+ or CD8+ or CD11b+ cells (using CD4-/- or CD8-/- or CD11b-/- knock-out mice) would be required.

In conclusion, with a specific experimental model simulating the clinical outcomes observed after radiotherapy, the present study underlines the importance of vascular dysfunction and collagen remodeling during both the acute and late phases of skin reaction to radiation. Further, BMMNC therapy in the early phase yielded more favorable collagen remodeling and vascular function, which helped to accelerate re-epithelialization and skin wound healing. More importantly, our work also suggests that the beneficial effects of BMMNC were maintained in the late phase and contributed to efficient control of vascular function without heightening the inflammatory response to irradiation. These observations may suggest that stem cell therapy based on BMMNC would be of major benefit for the treatment of radiological skin burns.

References

1. Carmeliet P. Angiogenesis in health and disease. Nat Med. 2003;9(6):653–660.
2. Li J, Zhang YP, Kirsner RS. Angiogenesis in wound repair: angiogenic growth factors and the extracellular matrix. Microsc Res Tech. 2003;60(1):107–114.
3. Jensen JM, Gau T, Schultze J, Lemmnitz G, Folster-Holst R, May T, Abels C, Proksch E. Treatment of acute radiodermatitis with an oil-in-water emulsion following radiation therapy for breast cancer: a controlled, randomized trial. Strahlenther Onkol. 2011;187(6):378–384.
4. McQuestion M. Evidence-based skin care management in radiation therapy: clinical update. Semin Oncol Nurs. 2011; 27(2):e1–e17.
5. Brown KR, Rzucidlo E. Acute and chronic radiation injury. J Vasc Surg. 2011;53(suppl 1):15S–21S.
6. François S, Mouiseddine M, Mathieu N, Semont A, Monti P, Dudoignon N, Saché A, Boutarfa A, Thierry D, Gourmelon P, Chapel A. Human mesenchymal stem cells favour healing of the cutaneous radiation syndrome in a xenogenic transplant model. Ann Hematol. 2007;86(1):1–8.
7. Wu Y, Wang J, Scott PG, Tredget EE. Bone marrow-derived stem cells in wound healing: a review. Wound Repair Regen. 2007;15(suppl 1):S18–S26.
8. Hill RP, Rodemann HP, Hendry JH, Roberts SA, Anscher MS. Normal tissue radiobiology: from the laboratory to the clinic. Int J Radiat Oncol Biol Phys. 2001;49(2):353–365.
9. Orlic D, Kajstura J, Chimenti S, Jakoniuk I, Anderson SM, Li B, Pickel J, McKay R, Nadal-Ginard B, Bodine DM, Leri A, Anversa P. Bone marrow cells regenerate infarcted myocardium. Nature. 2001;410(6829):701–705.
10. Kocher AA, Schuster MD, Szabolcs MJ, Takuma S, Burkhoff D, Wang J, Homma S, Edwards NM, Itescu S. Neovascularization of ischemic myocardium by human bone-marrow-derived angioblasts prevents cardiomyocyte apoptosis, reduces remodeling and improves cardiac function. Nat Med. 2001; 7(4):430–436.
11. Ebrahimian TG, Pouzoulet F, Squiban C, Buard V, Andre M, Cousin B, Gourmelon P, Benderitter M, Casteilla L, Tamarat R. Cell therapy based on adipose tissue-derived stromal cells promotes physiological and pathological wound healing. Arterioscler Thromb Vasc Biol. 2009;29(4):503–510.
12. Teraa M, Sprengers RW, Schutgens RE, Slaper-Cortenbach IC, van der Graaf Y, Algra A, van der Tweel I, Doevendans PA, Mali WP, Moll FL, Verhaar MC. Effect of repetitive intra-

arterial infusion of bone marrow mononuclear cells in patients with no-option limb ischemia: the randomized, double-blind, placebo-controlled Rejuvenating Endothelial Progenitor Cells via Transcutaneous Intra-arterial Supplementation (JUVEN-TAS) trial. Circulation. 2015;131(10):851–860.

13. Holler V, Buard V, Gaugler MH, Guipaud O, Baudelin C, Sache A, Perez Mdel R, Squiban C, Tamarat R, Milliat F, Benderitter M. Pravastatin limits radiation-induced vascular dysfunction in the skin. J Invest Dermatol. 2009;129(5):1280–1291.

14. Van der Meeren A, Mouthon MA, Vandamme M, Squiban C, Aigueperse J. Combinations of cytokines promote survival of mice and limit acute radiation damage in concert with amelioration of vascular damage. Radiat Res. 2004;161(5):549–559.

15. Fukumura D, Ushiyama A, Duda DG, Xu L, Tam J, Krishna V, Chatterjee K, Garkavtsev I, Jain RK. Paracrine regulation of angiogenesis and adipocyte differentiation during in vivo adipogenesis. Circ Res. 2003;93(9):e88–e97.

16. Metson R, Freehling DJ, Wang CC. Surgical complications following twice-a-day versus once-a-day radiation therapy. Laryngoscope. 1988;98(1):30–34.

17. Ormsby MV, Hilaris BS, Nori D, Brennan MF. Wound complications of adjuvant radiation therapy in patients with soft-tissue sarcomas. Ann Surg. 1989;210(1):93–99.

18. Bernstein EF, Salomon GD, Harisiadis L, Talbot T, Harrington F, Russo A, Uitto J. Collagen gene expression and wound strength in normal and radiation-impaired wounds. A model of radiation-impaired wound healing. J Dermatol Surg Oncol. 1993;19(6):564–570.

19. Iwahira Y, Nagase T, Nakagami G, Huang L, Ohta Y, Sanada H. Histopathological comparisons of irradiated and non-irradiated breast skin from the same individuals. J Plast Reconstr Aesthet Surg. 2012;65(11):1496–1505.

20. Gorodetsky R, McBride WH, Withers HR, Miller GG. Effect of fibroblast implants on wound healing of irradiated skin: assay of wound strength and quantitative immunohistology of collagen. Radiat Res. 1991;125(2):181–186.

21. Ferguson PC, Boynton EL, Wunder JS, Hill RP, O'Sullivan B, Sandhu JS, Bell RS. Intradermal injection of autologous dermal fibroblasts improves wound healing in irradiated skin. J Surg Res. 1999;85(2):331–338.

22. Lindbom L, Xie X, Raud J, Hedqvist P. Chemoattractant-induced firm adhesion of leukocytes to vascular endothelium in vivo is critically dependent on initial leukocyte rolling. Acta Physiol Scand. 1992;146(4):415–421.

23. Quarmby S, Kumar P, Kumar S. Radiation-induced normal tissue injury: role of adhesion molecules in leukocyte-endothelial cell interactions. Int J Cancer. 1999;82(3): 385–395.

24. Heckmann M, Douwes K, Peter R, Degitz K. Vascular activation of adhesion molecule mRNA and cell surface expression by ionizing radiation. Exp Cell Res. 1998;238(1):148–154.

25. Kimura H, Wu NZ, Dodge R, Spencer DP, Klitzman BM, McIntyre TM, Dewhirst MW. Inhibition of radiation-induced up-regulation of leukocyte adhesion to endothelial cells with the platelet-activating factor inhibitor, BN52021. Int J Radiat Oncol Biol Phys. 1995;33(3):627–633.

26. You D, Waeckel L, Ebrahimian TG, Blanc-Brude O, Foubert P, Barateau V, Duriez M, Lericousse-Roussanne S, Vilar J, Dejana E, Tobelem G, Lévy BI, Silvestre JS. Increase in vascular permeability and vasodilation are critical for proangiogenic effects of stem cell therapy. Circulation. 2006;114(4): 328–338.

27. Kubes P, Suzuki M, Granger DN. Nitric oxide: an endogenous modulator of leukocyte adhesion. Proc Natl Acad Sci U S A. 1991;88(11):4651–4655.

28. Lefer AM. Nitric oxide: nature's naturally occurring leukocyte inhibitor. Circulation. 1997;95(3):553–554.

29. Schaper W. Collateral circulation: past and present. Basic Res Cardiol. 2009;104(1):5–21.

30. Mees B, Recalde A, Loinard C, Tempel D, Godinho M, Vilar J, van Haperen R, Levy B, de Crom R, Silvestre JS. Endothelial nitric oxide synthase overexpression restores the efficiency of bone marrow mononuclear cell-based therapy. Am J Pathol. 2011;178(1):55–60.

31. Foubert P, Squiban C, Holler V, Buard V, Dean C, Levy BI, Benderitter M, Silvestre JS, Tobelem G, Tamarat R. Strategies to enhance the efficiency of endothelial progenitor cell therapy by ephrin B2 pretreatment and coadministration with smooth muscle progenitor cells on vascular function during the wound-healing process in irradiated or nonirradiated condition. Cell Transplant. 2015;24(7):1343–1361.